



HAL
open science

Permutation entropy-derived parameters to estimate the epileptogenic zone network

Ionuț-Flavius Bratu, Julia Makhalova, Elodie Garnier, Samuel Medina Villalon, Aude Jegou, Francesca Bonini, Stanislas Lagarde, Francesca Pizzo, Agnès Trébuchon, Didier Scavarda, et al.

► To cite this version:

Ionuț-Flavius Bratu, Julia Makhalova, Elodie Garnier, Samuel Medina Villalon, Aude Jegou, et al.. Permutation entropy-derived parameters to estimate the epileptogenic zone network. *Epilepsia*, 2023, 65 (2), pp.389-401. 10.1111/epi.17849 . hal-04793774

HAL Id: hal-04793774

<https://hal.science/hal-04793774v1>

Submitted on 20 Nov 2024

HAL is a multi-disciplinary open access archive for the deposit and dissemination of scientific research documents, whether they are published or not. The documents may come from teaching and research institutions in France or abroad, or from public or private research centers.






L'archive ouverte pluridisciplinaire **HAL**, est destinée au dépôt et à la diffusion de documents scientifiques de niveau recherche, publiés ou non, émanant des établissements d'enseignement et de recherche français ou étrangers, des laboratoires publics ou privés.



Distributed under a Creative Commons Attribution - NonCommercial - NoDerivatives 4.0 International License

RESEARCH ARTICLE

Permutation entropy-derived parameters to estimate the epileptogenic zone network

Ionuț-Flavius Bratu^{1,2}  | Julia Makhalova^{1,2,3}  | Elodie Garnier²  |
 Samuel Medina Villalon^{1,2} | Aude Jegou² | Francesca Bonini^{1,2} | Stanislas Lagarde^{1,2}  |
 Francesca Pizzo^{1,2} | Agnès Trébuchon^{1,2}  | Didier Scavarda^{1,4}  | Romain Carron^{1,5} |
 Christian Bénar²  | Fabrice Bartolomei^{1,2} 

¹APHM, Timone Hospital, Epileptology and Cerebral Rhythmology, Marseille, France

²Aix Marseille Univ, INSERM, INS, Inst Neurosci Syst, Marseille, France

³APHM, Timone Hospital, CEMEREM, Marseille, France

⁴APHM Paediatric Neurosurgery Department, Marseille, France

⁵APHM Functional Neurosurgery Department, Marseille, France

Correspondence

Fabrice Bartolomei, Service d'Epileptologie et de Rythmologie cérébrale, Hôpital Timone, 264 Rue Saint-Pierre, 13005 Marseille, France.
 Email: fabrice.bartolomei@ap-hm.fr

Funding information

Agence Nationale de la Recherche, Grant/Award Number: ANR-17-RHUS-0004; H2020 European Research Council, Grant/Award Number: 855109

Abstract

Objective: Quantification of the epileptogenic zone network (EZN) most frequently implies analysis of seizure onset. However, important information can also be obtained from the postictal period, characterized by prominent changes in the EZN. We used permutation entropy (PE), a measure of signal complexity, to analyze the peri-ictal stereoelectroencephalography (SEEG) signal changes with emphasis on the postictal state. We sought to determine the best PE-derived parameter (PEDP) for identifying the EZN.

Methods: Several PEDPs were computed retrospectively on SEEG-recorded seizures of 86 patients operated on for drug-resistant epilepsy: mean baseline preictal entropy, minimum ictal entropy, maximum postictal entropy, the ratio between the maximum postictal and the minimum ictal entropy, and the ratio between the maximum postictal and the baseline preictal entropy. The performance of each biomarker was assessed by comparing the identified epileptogenic contacts or brain regions against the EZN defined by clinical analysis incorporating the Epileptogenicity Index and the connectivity epileptogenicity index methods (EZN_C), using the receiver-operating characteristic and precision-recall.

Results: The ratio between the maximum postictal and the minimum ictal entropy (defined as the Permutation Entropy Index [PEI]) proved to be the best-performing PEDP to identify the EZN_C. It demonstrated the highest area under the curve (AUC) and F1 score at the contact level (AUC 0.72; F1 0.39) and at the region level (AUC 0.78; F1 0.47). PEI values gradually decreased between the EZN, the propagation network, and the non-involved regions. PEI showed higher performance in patients with slow seizure-onset patterns than in those with fast seizure-onset patterns. The percentage of resected epileptogenic regions defined by PEI was significantly correlated with surgical outcome.

Christian Bénar and Fabrice Bartolomei contributed equally to this work.

This is an open access article under the terms of the [Creative Commons Attribution-NonCommercial-NoDerivs](https://creativecommons.org/licenses/by-nc-nd/4.0/) License, which permits use and distribution in any medium, provided the original work is properly cited, the use is non-commercial and no modifications or adaptations are made.

© 2023 The Author(s). *Epilepsia* published by Wiley Periodicals LLC on behalf of International League Against Epilepsy.

Significance: PEI is a promising tool to improve the delineation of the EZN. PEI combines ease and robustness in a routine clinical setting with high sensitivity for seizures without fast activity at seizure onset.

KEYWORDS

permutation entropy index, postictal, SEEG, signal complexity

1 | INTRODUCTION

Epilepsy surgery is an effective treatment option for patients with focal drug-resistant epilepsy.¹ Classically, surgery aims at removing or disconnecting the seizure-generating brain regions, called the epileptogenic zone (EZ). In many cases, the localization and electro-anatomic definition of these areas requires invasive electroencephalography (EEG) recordings. In this context, stereo-EEG (SEEG) is the reference method.^{2,3} Numerous studies have shown that focal epilepsies are network diseases characterized by alterations in excitability and connectivity affecting specific neural networks.^{4,5} Using SEEG signal quantification approaches, it has been demonstrated that the epileptogenic networks are hierarchically organized into the epileptogenic zone network (EZN), the propagation zone network (PZN), and the non-involved networks (NIZ).⁵ The EZN is the surgical target and is conceptualized as a network of hyperexcitable connected brain regions capable of generating seizures that secondarily involve the PZN. Quantification methods have been proposed to better define the SEEG seizure-generating regions and facilitate the interpretation.⁶ The first method described for this purpose was the epileptogenicity index (EI),⁷ based on estimating a combination of the increase in fast frequencies and of delays of involvement of brain regions. Other methods have been described subsequently,⁸⁻¹¹ most often being based on the detection of rapid activities that are present during seizure onset in ~75% of the cases.^{12,13} Besides a better comprehension/description of the underlying process, these methods could contribute to improving SEEG interpretation and to address the current challenges of epilepsy surgery outcome (60% seizure-freedom rate in SEEG-based surgical series^{12,14,15}). These quantification approaches typically analyze SEEG signals during the preictal-ictal transition. It is worth noting that valuable insights can be gained from observing the entire seizure process, including the pre-ictal period¹⁶ and the post-ictal period, which is typically marked by significant changes (flattening, slowing) in the regions responsible for generating seizures.^{6,17}

In this study, we analyzed the dynamics of ictal and peri-ictal SEEG signals including the postictal state using permutation entropy (PE) in patients who underwent

Key points

- Permutation entropy is an effective method for estimating the epileptogenic zone network using ictal and post-ictal signal properties.
- Permutation Entropy Index (PEI) is the ratio between the maximum postictal and the minimum ictal entropy.
- PEI was the best-performing parameter in detecting epileptogenic regions as compared against current clinical and quantification approaches.
- PEI is particularly advantageous for the cases without fast activity at seizure onset.
- The percentage of resected epileptogenic regions defined by PEI correlated with surgical outcome.

SEEG and surgery. Entropy quantifies signal complexity by estimating the degree of uncertainty associated with the probability distribution of the EEG time series.^{18,19}

We aimed to find the best-performing PE-derived parameter (PEDP) for identifying the EZN as defined by a clinical analysis incorporating quantifying methods that our team uses in routine: the EI⁷ and the connectivity epileptogenicity index (cEI).⁸

2 | MATERIALS AND METHODS

2.1 | Patients and data acquisition

PE quantification was performed on the SEEG recordings of a retrospective cohort of 86 patients with focal drug-resistant epilepsy who underwent presurgical assessment followed by surgery at La Timone Hospital in Marseille between 2008 and 2020. All consecutive patients with available SEEG recordings of at least two spontaneous seizures (each data set including 60s of preictal and 60s of postictal period), post-surgical brain magnetic resonance imaging (MRI), and a minimum of 1 year of postsurgical follow-up were included.

Presurgical assessment included detailed medical history, neurological examination, neuropsychological testing, 3T MRI, fluorodeoxyglucose–positron emission tomography (FDG-PET), long-term scalp video-EEG, and SEEG recordings in all included patients. Surgical outcome was assessed according to Engel classification at the last clinical follow-up. All patients have given informed written consent, and this study was approved by the Assistance Publique – Hôpitaux de Marseille (PADS23-41).

2.2 | SEEG exploration

In all patients, SEEG explorations were performed as a part of routine presurgical assessment in line with the French national guidelines.²⁰ Intracerebral electrodes (10–19 contacts per electrode, 2 mm contact length, 1.5 mm contact spacing, and 0.8 mm diameter, Dixi or Alcis) were implanted according to the Talairach stereotactic³ until 2017 and using the ROSA robotic surgical assistant in adults²¹ or a frameless neuronavigation method²² in children thereafter. Signals were recorded on a 128- or 256-channel Natus system, sampled at 512 or 1024 Hz, and saved on a hard disk (16 bits/sample) using no digital filter. Two hardware filters were present in the acquisition procedure: a high-pass filter (cutoff frequency equal to 1 Hz at –3 dB) and an anti-aliasing low-pass filter (cutoff frequency equal to 170 Hz at 512 Hz, or 340 Hz at 1024 Hz).

All signal analyses were performed in a bipolar montage using the open-source AnyWave software²³ available at <https://meg.univ-amu.fr/wiki/AnyWave>. For each patient, a bipolar montage including all contacts within the gray matter was automatically generated using GARDEL software.²⁴ Co-registration of the pre-implantation T1-MRI with post-implantation computed tomography (CT) images was performed, followed by an automatic recognition and anatomic localization of each electrode contact, which was then assigned automatically to the respective anatomic region of the virtual epileptic patient (VEP) atlas²⁵ projected in the patient's MRI space.²⁴ Channels containing artifacts were excluded by visual inspection. Seizure-onset patterns (SOPs) were assessed using the methodology described previously¹² and were divided into fast-onset patterns (characterized by the presence of low-voltage fast activity >14 Hz within the first 10 s from seizure onset) and slow onset patterns (without low-voltage fast activity within the first 10 s from seizure onset).

2.3 | SEEG signal analysis and permutation entropy estimation

The same SEEG data sets and montages of each respective patient were used for the visual analysis and for the

quantification of ictal epileptogenicity markers (EI and cEI), as well as the PEDPs. At least two spontaneous seizures per patient were analyzed. If two or more seizure types were present, at least one representative seizure of each type was analyzed. For the whole cohort, a total of 203 seizures with 82.5 ± 29.2 bipolar channels per data set were analyzed.

The epileptogenic regions were defined by three expert clinicians (I.F.B., J.M., and F.B.), based on visual and quantitative SEEG-signal analysis using the EI⁷ and the cEI⁸ methods.

EI and cEI were computed on the same seizures and using the same montages as employed when operating the Entropy plugin (See details in Appendix S1: Methods). A dedicated Matlab plug-in was used (EI/cEI plug-in, <https://meg.univ-amu.fr/wiki/AnyWave:Plug-ins>) to compute both markers simultaneously. In each patient and for each bipolar channel, the maximal normalized EI and the maximal cEI values from all the analyzed seizures were computed.

Previous studies using EEG/SEEG signals have shown that changes in entropy may reflect the seizure dynamics, in particular a decrease during seizures^{26,27} and an increase in the immediate post-ictal period.²⁸ We have leveraged this characteristic to track the alterations that occur during seizures recorded by SEEG.

PE is based on the Shannon entropy²⁹ for quantifying the probability distribution of ordinal patterns determined by the order relations between equidistant values of a time series.^{27,30} Starting from a one-dimensional time series $S(t) = x_t$; $t = 1 \dots T$, a set of D vectors is created, where D represents the embedding dimension that determines how many samples of the signal are contained in each vector. The values contained in each vector are consecutive points x_t separated by a fixed time delay τ measured in samples ($\tau = 1$ for consecutive samples). Each vector of signal samples is then assigned an ordinal pattern π that corresponds to the ranks of amplitudes within the vector. For example, signals samples [3.4 4.1 2.5] (embedding dimension of 3) would give an ordinal pattern [2 3 1] (the corresponding ranks in the vector of samples). In a second step, the probability $p(\pi)$ of the occurrence of a certain ordinal pattern π within a given time window is computed. The entropy in the window is then defined as $H(D) = -\frac{1}{\log_2 D!} \sum p(\pi) \log_2(p(\pi))$. The values of $H(D)$ range between 0 and 1; the smaller the value the more regular and more deterministic the time series is, with 0 meaning that the signal is perfectly organized (there is only one ordinal pattern), the closer to 1 the more noisy and random the time series, and 1 meaning completely disorganized (all the ordinal patterns have equal probability, e.g., completely random noise).³¹

To perform PE analysis of the SEEG signals, a dedicated Matlab plug-in based on the algorithm developed by

Unakafova et al. was used.³² Based on exploratory trials and a review of the literature, the PE analysis parameters employed were $D=3$ (embedding dimension/PE of order 3) and a time delay $\tau=1$, using a sliding time window of 5s with an overlap of 2.5s.

The duration of preictal and postictal periods used for the PEDPs computation was empirically set to 60s before the visual seizure onset and 60s after the visual seizure offset (Figure 1A), based on the observed signal dynamics (Figure 1B), the length of available SEEG data sets, and the time required for data pre-processing.

The following PEDPs were computed:

- the mean PE of the baseline signal before the visual seizure onset (B);
- the minimum PE of the signal between the visual seizure onset and seizure offset (m);
- the maximum PE of the signal after the visual seizure offset (M);
- the ratio between the maximum postictal entropy and the minimum ictal entropy ($\frac{M}{m}$); and
- the ratio between the maximum postictal entropy and the baseline preictal entropy ($\frac{M}{B}$).

In all further computation, normalized PEDP values were used, that is, the absolute value of each marker obtained at the respective bipolar channel divided by the maximum value among all channels for each seizure. In each patient and for each bipolar channel, the maximal or minimal normalized PEDPs values from all the analyzed seizures were computed: M_{\max} , m_{\min} , $\frac{M}{m}_{\max}$ and $\frac{M}{B}_{\max}$.

2.4 | Definition of regions of interest

In the present study, the regions of interest (ROIs) were defined at two levels: (1) the bipolar SEEG contacts within the gray matter (corresponding to the montage used for the analyses in each patient), and (2) the brain regions defined according to the VEP atlas parcellation,²⁵ available at <https://ins-amu.fr/vep-atlas>. To obtain correspondence between the SEEG contacts and the brain regions, each electrode contact was assigned automatically by GARDEL software²⁴ to the respective anatomic region of the VEP atlas projected in the patient's MRI space.

Three expert clinicians (I.F.B., J.M., and F.B.) labeled each bipolar SEEG contact as belonging to the EZN,

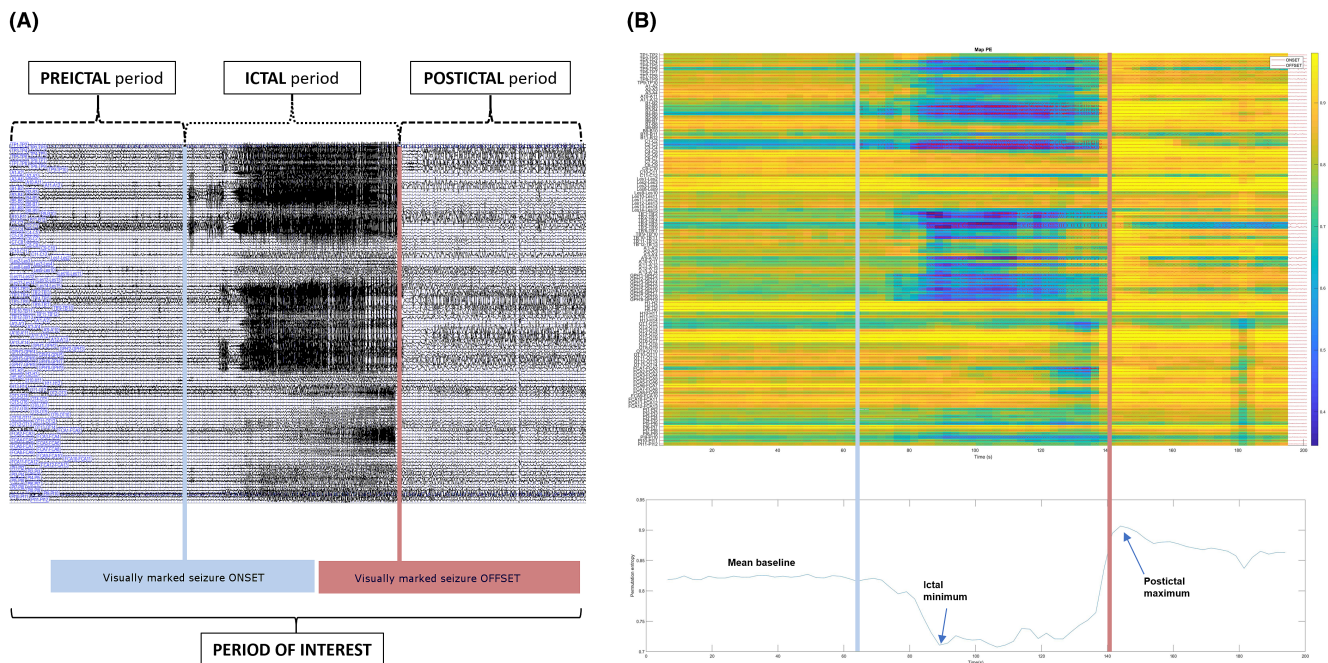


FIGURE 1 Permutation entropy computation steps and peri-ictal dynamics. (A) Example of visual marking of the electrical seizure onset (ONSET) and termination (OFFSET). The considered period of interest comprises a part of the preictal period (starting 60s before the ONSET marker, blue), the ictal period (between the ONSET and OFFSET markers), and a part of the postictal period (finishing 60s after the OFFSET marker, pink). (B) Trend of complexity during the period of interest as highlighted by the permutation entropy analysis of the same seizure as in (A). The blue vertical bar marks seizure onset and the pink vertical bar marks the seizure termination. The upper image shows a colored map representation of entropy changes in the SEEG signal for each bipolar channel. The lower image illustrates the global entropy trend of all channels. The mean baseline signal complexity decreases at seizure onset and reaches an ictal minimum. The complexity starts to increase toward the electrical end of the seizure and continues to increase even after it reaches a post-ictal peak and plateau higher than the baseline complexity.

PZN, or NIZ based on the clinical analysis incorporating the EI and cEI methods. A visual inspection of ictal (in the present study only spontaneous seizures) and interictal SEEG recordings was performed. Seizure onset was defined as the first change of SEEG signal within the context of a sustained rhythmic discharge and subsequent appearance of clinical signs.⁶ The discrepancies in interpretation were solved through the collegial decision between the clinical experts. Using validated thresholds³³ for EI and cEI, contacts with $EI \geq 0.4$ and/or $cEI \geq 0.65$ were defined as the EZN; contacts with $0.1 < EI < 0.4$ and/or $0.3 < cEI < 0.65$ and sustained discharge during the seizure were defined as the PZN; all other contacts were defined as the NIZ. In the same way, each brain region was labeled as the EZN, PZN, or NIZ, based on the definition used for the bipolar contacts that sampled the respective regions.

The above-described labeling of SEEG contacts and brain regions according to the clinical analysis incorporating the EI and cEI was defined as clinical hypothesis (EZNC/PZNC/NIZC) for further analysis.²¹

For each PEDP, a threshold has been established (see below) above which the respective SEEG contact was defined as epileptogenic (EZNP_{PE}); all contacts with PEDP values below the threshold were defined as non-EZNP_{PE}. In the same way, the corresponding brain regions were defined as EZNP_{PE} or non-EZNP_{PE} for further analysis.

In a subgroup of 54 patients, resected and non-resected contacts and brain regions were estimated by visual inspection using GARDEL software according to the methodology described in.²¹ In brief, the co-registration of the post-implantation CT with electrodes with the post-operative MRI, and that of the post- and pre-operative MRI were performed; resected contacts and VEP Atlas regions were identified by visual inspection (S.M.V. and J.M.). For all ROIs, a “resected” or “non-resected” status was assigned. A brain region was considered resected if at least 50% of its major axis length was operated on.

2.5 | Statistical analysis

Statistical analyses were performed using R³⁴ and Prism (GraphPad Software Inc). Receiver-operating characteristic (ROC) and precision-recall (PR) curves were computed first at the patient level and then at the cohort level for the whole cohort, as well as the Engel I (seizure-free, Engel class I), the Engel non-I (non-seizure-free, Engel classes II–III), the slow SOP, and the fast SOP patient subgroups. The EZNC was used as ground truth, and a set of thresholds were applied to the PEDPs to define the EZNP_{PE}/non-EZNP_{PE} using the subgroup of 41 seizure-free patients (Engel class I), assuming that our reference, the EZNC,

was defined correctly in these patients. The performances of the different PEDPs in correctly identifying a contact or region as being part of the EZNC were compared to find the best entropy-based classifier. We also computed the area under the ROC curve (AUC) to evaluate the relevance of each ROC curve. For PR curves, we used the F1 score as the evaluation metric. Independent sample tests (Student's *t* test or Mann-Whitney *U*) were used to assess group differences in terms of the maximal (or minimal) PEDP. One-way analysis of variance (ANOVA) was used to measure the difference between groups with more than two categories. Spearman rank correlation was used to examine covariance between the PEDP values and other variables. For details see Appendix S2: Statistical Analysis.

3 | RESULTS

3.1 | Cohort description

Patients' clinical characteristics are summarized in Table 1. Eighty-six patients (34 male, 52 female) were included. The mean age at epilepsy onset was 12 years (first day of life–55 years), the mean epilepsy duration at the time of SEEG exploration was 12.87 years (1.3–56.1), and the mean epilepsy duration at the time of surgery was 14.07 years (1.7–56.7). The EZNC was unilateral in 82 cases and bilateral in 4 cases. The EZNC topography was temporal in 37 patients (43%), temporal plus in 20 patients (23%), extratemporal in 28 patients (33%), and hemispheric in 1 patient. Fast SOP were observed in 67 patients (78%), slow SOP in 24 patients (28%), and mixed SOP (EZNC contacts within different structures exhibiting either fast or slow SOP) in 5 patients (6%). Noteworthy, in some patients, both fast and slow SOP could be observed in different seizures. An MRI-visible lesion was present in 80% of cases. The mean post-surgical follow-up period was 5.54 years (2.1–12.9). Post-surgical outcome was Engel class I in 41 patients (48%), Engel class II in 9 patients (10%), Engel class III in 17 patients (20%), and Engel class IV in 19 patients (22%). The most common histopathological findings were focal cortical dysplasia in 28% and hippocampal sclerosis in 15% of cases.

3.2 | Performances of different PEDPs in estimating the EZNC

We observed a decrease in signal entropy (complexity) at seizure onset compared to baseline, the minimum being reached during the ictal period. Moreover, in most seizures, we noted that the complexity starts to increase toward the electrical termination of the seizure

Sex, male/female, <i>n</i>	34/52
Age at epilepsy onset, years, mean \pm SD (range)	12.00 \pm 11.87 (0–55)
Epilepsy duration until SEEG, years, mean \pm SD (range)	12.87 \pm 10.89 (1.3–56.1)
Epilepsy duration until surgery, years, mean \pm SD (range)	14.07 \pm 11.01 (1.7–56.7)
Epilepsy type, localization of the epileptogenic zone, % (<i>n</i>)	
Temporal	43% (37)
Lateral	7% (5)
Mesial	31% (27)
Lateral–mesial	6% (5)
Temporal plus	23% (20)
Frontal-temporal	10% (9)
Frontal-temporal-insular	3% (3)
Temporal-insular	5% (4)
Temporal–parietal	1% (1)
Temporal-occipital	2% (2)
Temporal–parietal-occipital	1% (1)
Extra-temporal	33% (28)
Frontal	17% (15)
Frontal-insular	1% (1)
Frontal–parietal	2% (2)
Frontal–parietal-insular	5% (4)
Insular	2% (2)
Parietal	2% (2)
Occipital	2% (2)
Hemispheric	1% (1)
Epilepsy side, % (<i>n</i>)	
Left	47% (40)
Right	49% (42)
Bilateral	5% (4)
Seizure-onset pattern, % (<i>n</i>)	
Fast	78% (67)
Slow	28% (24)
Mixed	6% (5)
Brain MRI, % (<i>n</i>)	
Normal	20% (17)
Lesional	80% (69)
Surgery, % (<i>n</i>)	
Resection	89% (76)
Disconnection	9% (8)
Gamma knife	2% (2)
Outcome, Engel class, % (<i>n</i>)	
I	48% (41)
II	10% (9)
III	20% (17)
IV	22% (19)

TABLE 1 Clinical characteristics of the patients.

and continues to increase even after, reaching a post-ictal peak and plateau higher than the baseline values (Figure 1B).

We compared the ROI identified as epileptogenic by different PEDPs (EZN_{PE}) against the EZN_C by using ROC as well as PR. The results of the whole cohort of 86 patients are summarized in Table 2. The thresholds allowing the best match with clinical analysis and optimized on the seizure-free sub-cohort are indicated for each evaluated PEDP and for each statistical method (ROC and PR), respectively.

The maximal normalized ratio between the maximum postictal entropy and the minimum ictal entropy ($\frac{M}{m_{max}}$) demonstrated the best performances in detecting the EZN_C , both at the SEEG contact level (AUC 0.72 and F1 score 0.39) and at the region level (AUC 0.78 and F1 score 0.47). In the following, we will call $\frac{M}{m_{max}}$ the permutation entropy index (PEI).

PEI disclosed decreasing values, both for the SEEG contacts and the brain regions, between the clinically defined EZN, PZN, and NIZ, respectively, confirming its relationship with epileptogenicity: PEI values were higher in the EZN_C than in the PZN_C or the NIZ_C ($p < .0001$), and higher in the PZN_C than the NIZ_C ($p < .01$) (Figure 2A).

3.3 | PEI performances depending on the seizure-onset pattern

Assessment of PEDP performances according to the SOP subgroups confirmed the PEI as being the best PEDP in identifying the EZN_C (Tables S1 and S2). When comparing the performances between the seizures with fast SOP and slow SOP, the PEI showed higher performances, in particular higher sensitivity (Sn), specificity (Sp), and precision in the slow SOP group compared to the fast SOP group. At SEEG contact level, PEI showed AUC of 0.77 (Sn 72%, Sp 72%) and F1 of 0.47 (precision 0.4, recall 0.59) in the slow SOP group vs AUC of 0.72 (Sn 66%, Sp 66%) and F1 of 0.39 (precision 0.29, recall 0.6) in the fast SOP group. This difference was even more prominent at the region level, where the PEI reached AUC of 0.85 (Sn 88%, Sp 71%) and an F1 score of 0.58 (precision 0.57, recall 0.6) in the slow SOP group vs AUC of 0.75 (Sn 76%, Sp 66%) and F1 of 0.46 (precision 0.33, recall 0.74) in the fast SOP group. This difference in the PEI performances between the slow-SOP and fast-SOP groups was statistically significant ($p < .05$) at the region level. However, there was no statistically significant difference between the two SOP groups at the contact level ($p > .05$).

TABLE 2 Performance of Permutation Entropy-Derived Parameters in detecting the clinically defined Epileptogenic Zone Network.

Parameter	Receiver-operating characteristic				Precision-recall			
	Threshold	AUC	Sn (%)	Sp (%)	Threshold	F1	Precision	Recall
Contact level								
M	0.92	0.6	56	63	0.92	0.33	0.23	0.56
M_{max}	0.93	0.63	66	54	0.93	0.32	0.21	0.65
m	0.65	0.66	64	62	0.63	0.36	0.26	0.59
m_{min}	0.61	0.66	64	60	0.56	0.33	0.25	0.52
$\frac{M}{m}$	0.63	0.72	73	59	0.67	0.39	0.28	0.64
$\frac{M}{m_{max}}$ (PEI)	0.68	0.72	73	60	0.72	0.39	0.29	0.62
$\frac{M}{B}$	0.77	0.62	67	48	0.80	0.32	0.22	0.59
$\frac{M}{B_{max}}$	0.81	0.64	66	52	0.82	0.31	0.21	0.62
Region level								
M_{max}	0.96	0.66	66	56	0.97	0.35	0.25	0.60
m_{min}	0.52	0.71	63	68	0.50	0.40	0.31	0.55
$\frac{M}{m_{max}}$ (PEI)	0.77	0.78	73	71	0.80	0.47	0.37	0.63
$\frac{M}{B_{max}}$	0.86	0.72	70	62	0.87	0.41	0.30	0.67

Note: Definition of the permutation entropy-derived parameters: M , maximal entropy value of the signal after the visual seizure-offset; M_{max} , maximum of M at patient level, taking into account all the analyzed seizures of that patient; m , minimum entropy value of the signal between the visual seizure onset and seizure offset; m_{min} , minimum of m at patient level, taking into account all the analyzed seizures of that patient; $\frac{M}{m}$, ratio between M and m ; $\frac{M}{m_{max}}$, maximum of $\frac{M}{m}$ at patient level, taking into account all the analyzed seizures of that patient; PEI, Permutation Entropy Index; $\frac{M}{B}$, ratio between M and B ; $\frac{M}{B_{max}}$, maximum of $\frac{M}{B}$ at patient level, taking into account all the analyzed seizures of that patient.

Abbreviations: AUC, area under the ROC (receiver-operating characteristic) curve; PEI, permutation entropy index; Sn, sensitivity (defined by ROC); Sp, specificity (defined by ROC).

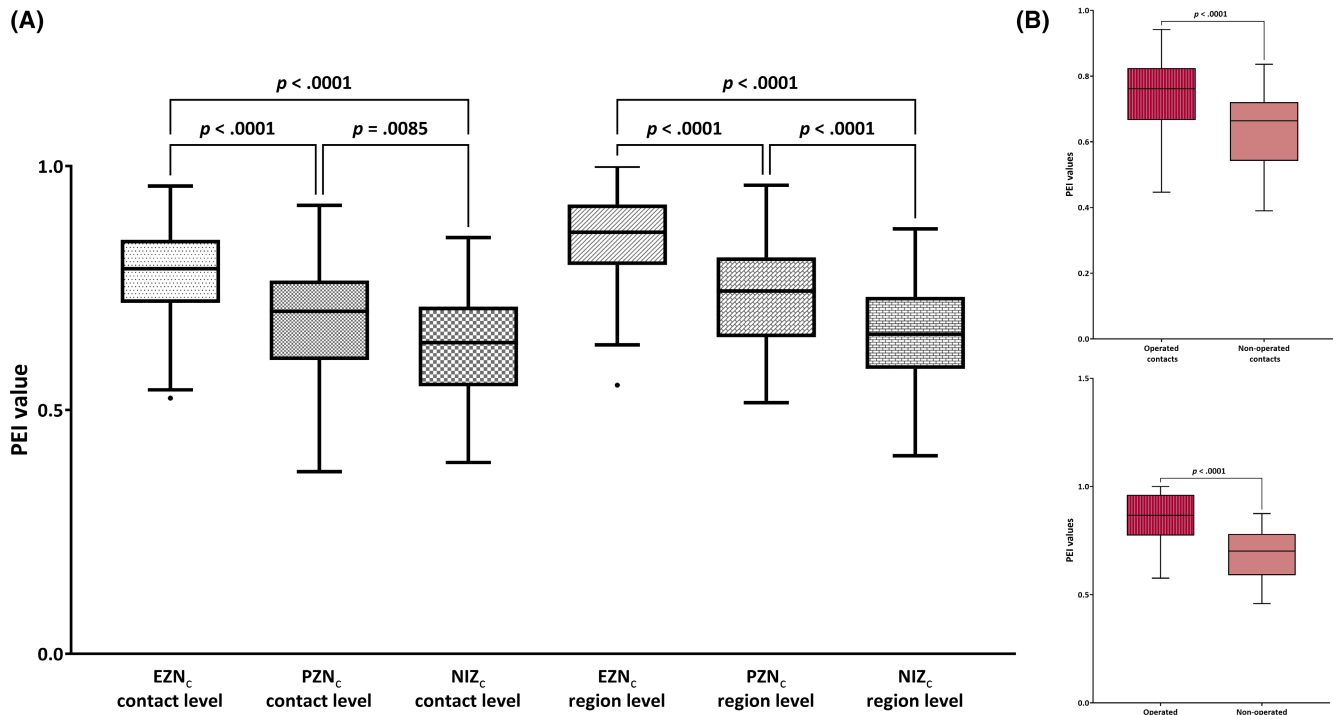


FIGURE 2 Permutation entropy index (PEI) with regard to the hierarchy of the epileptogenic networks and the surgical resection. (A) PEI values in the clinically defined epileptogenic, propagation, and non-involved zone networks at contact and region level. (B) PEI values were higher in the resected than in the non-resected contacts and regions. EZN_c, Epileptogenic Zone Network; NIZ_c, Non-involved Zone Network; PEI, Permutation Entropy Index; PZN_c, Propagation Zone Network. The EZN_c, PZN_c, and NIZ_c are defined according to the clinical analysis incorporating the EI and cEI methods.

3.4 | PEI performances and surgical outcome

When comparing the performances between the Engel I and Engel non-I patient groups, the PEI tended to show better performance scores, with higher sensitivity (ROC), higher recall (PR), and slightly better precision in the Engel I group (Table S3). However, these differences between the Engel I and Engel non-I groups were not statistically significant ($p > .05$), neither at the contact level nor at the region level.

Two clinical use cases showing the performance of different PEDPs are illustrated in Figure 3 and Figure S1.

3.5 | PEI with regard to the surgical resection

Resected and non-resected contacts and brain regions were estimated in 54 patients. Globally, PEI values were higher in the resected than in the non-resected contacts and regions ($p < .0001$, Figure 2B). Furthermore, we compared the extent of the EZN resection for the EZN_c and the EZN_{PE} defined by the PEI between the Engel I and the Engel non-I patient groups. Of note, the EZN_{PE} was

defined by the PEI value thresholds established using the Engel I group (see Methods): for the ROC analysis 0.68 (contact level) and 0.77 (region level) and for the PR analysis 0.72 (contact level) and 0.80 (region level). The extent of the EZN_c resection was greater in the Engel I group than in the Engel non-I group, both for the resected contacts and regions ($p < .01$, Figure 4A). In the same way, the percentage of resected EZN_{PE} contacts and regions was significantly higher in the Engel I group than in the Engel non-I group ($p < .05$, both ROC and PR-based thresholds, Figure 4B). Accordingly, the percentage of non-resected EZN_{PE} contacts and regions was significantly higher in the Engel non-I group ($p < .05$, both ROC and PR-based thresholds, Figure 4C). However, the number of non-resected EZN_{PE} contacts and regions identified by the PEI, but not defined as epileptogenic by the clinical analysis incorporating the EI and cEI methods did not differ between the Engel I and Engel non-I groups ($p > .05$, Figure 4D).

3.6 | Correlation between PEI and clinical variables

There was no correlation between the PEI values in the EZN_c, PZN_c, or NIZ_c and the age at epilepsy onset or

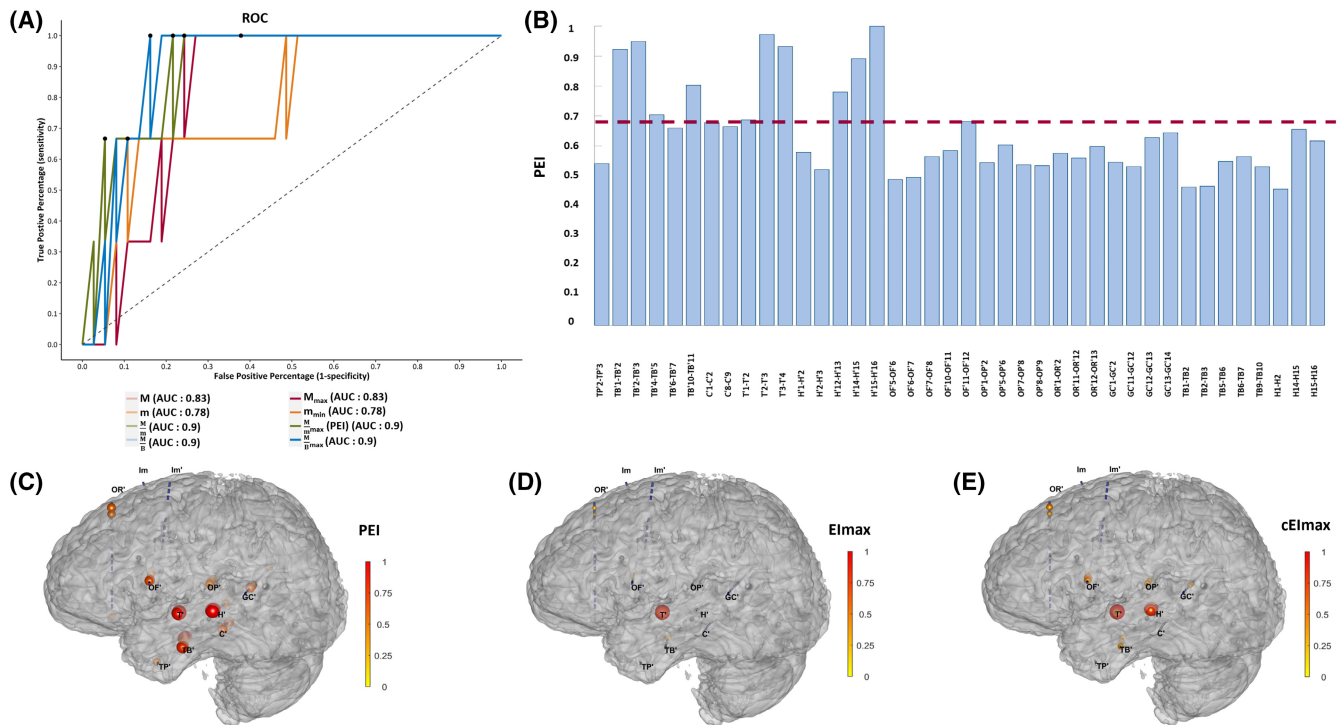


FIGURE 3 Illustrative case of Engel I patient. A 36-year-old right-handed female patient with drug-resistant epilepsy associated with a left temporal lateral ganglioglioma. The EZNC included the left anterior T1 (perilesional cortex sampled by the electrode T', just posterior to the lesion) up to Heschl gyrus (the electrode H'), the temporal pole, the amygdala, and the anterior hippocampus. The resection of these structures sparing the hippocampus (high risk of verbal memory impairment) led to a sustained seizure freedom (Engel class I at 3-years follow-up). The PEI was concordant with clinical analysis incorporating EI and cEI, and additionally identified the left T2 anterior. (A) ROC curves showing performances of PEDPs in identifying the EZNC channels. (B) Bar plot showing the PEI values quantified for the bipolar SEEG channels (two channels located within the gray matter and with good signal quality per each region are shown). The PEI epileptogenicity threshold is indicated by a red dotted line. (C) PEI values, EI (D), and cEI (E) values projected on the patient's 3D brain mesh. cEI, connectivity epileptogenicity index; EI, Epileptogenicity Index; EZNC, Epileptogenic Zone Network defined according to the clinical analysis incorporating the EI and cEI methods; PEDP, Permutation Entropy Derived Parameter; PEI, Permutation Entropy Index; ROC, Receiver-Operating Characteristic; SEEG, stereo-electroencephalography.

epilepsy duration. There was a positive correlation between the PEI values in the NIZ_C and epilepsy duration until the SEEG exploration ($\rho = 0.223$, $p = .039$).

4 | DISCUSSION

The search for epileptogenicity biomarkers is an important goal to improve the interpretation and guide surgical indication of SEEG presurgical exploration. Most current quantification methods and biomarkers attempt to achieve this goal by focusing on pre-ictal and ictal states. However, the analysis of post-ictal state can provide an important additional information. We demonstrate that the PEI is an effective and easily applicable method for estimating EZN using both ictal and post-ictal properties.

In this study, we proposed to quantify the EZN by using PE, a measure of signal complexity, taking into account the dynamic of changes from the seizure onset

to the post-ictal period. Permutation entropy overcomes the drawbacks of the classical methods of non-linear dynamics analysis.³⁵ Other entropy estimators ignore the temporal order in a time series (e.g., Shannon entropy) or require very long time series while being computationally expensive (e.g., Kolmogorov-Sinai entropy).^{36,37}

We observed a decrease in signal complexity at seizure onset compared to baseline, the minimum being reached during the ictal period. Our findings are concordant with previous intracranial EEG (iEEG) findings indicating a decrease in complexity observed during the ictal state in the seizure onset areas, whereas brain areas recruited during seizure spread showed less complexity reduction.^{38,39} Epileptogenic regions also disclose marked SEEG signal changes during the post-ictal period, mainly characterized by an increase in the entropy of the SEEG signal. This increase in entropy could be interpreted as abnormal complexity close to a stochastic random signal. It is likely that the information contained

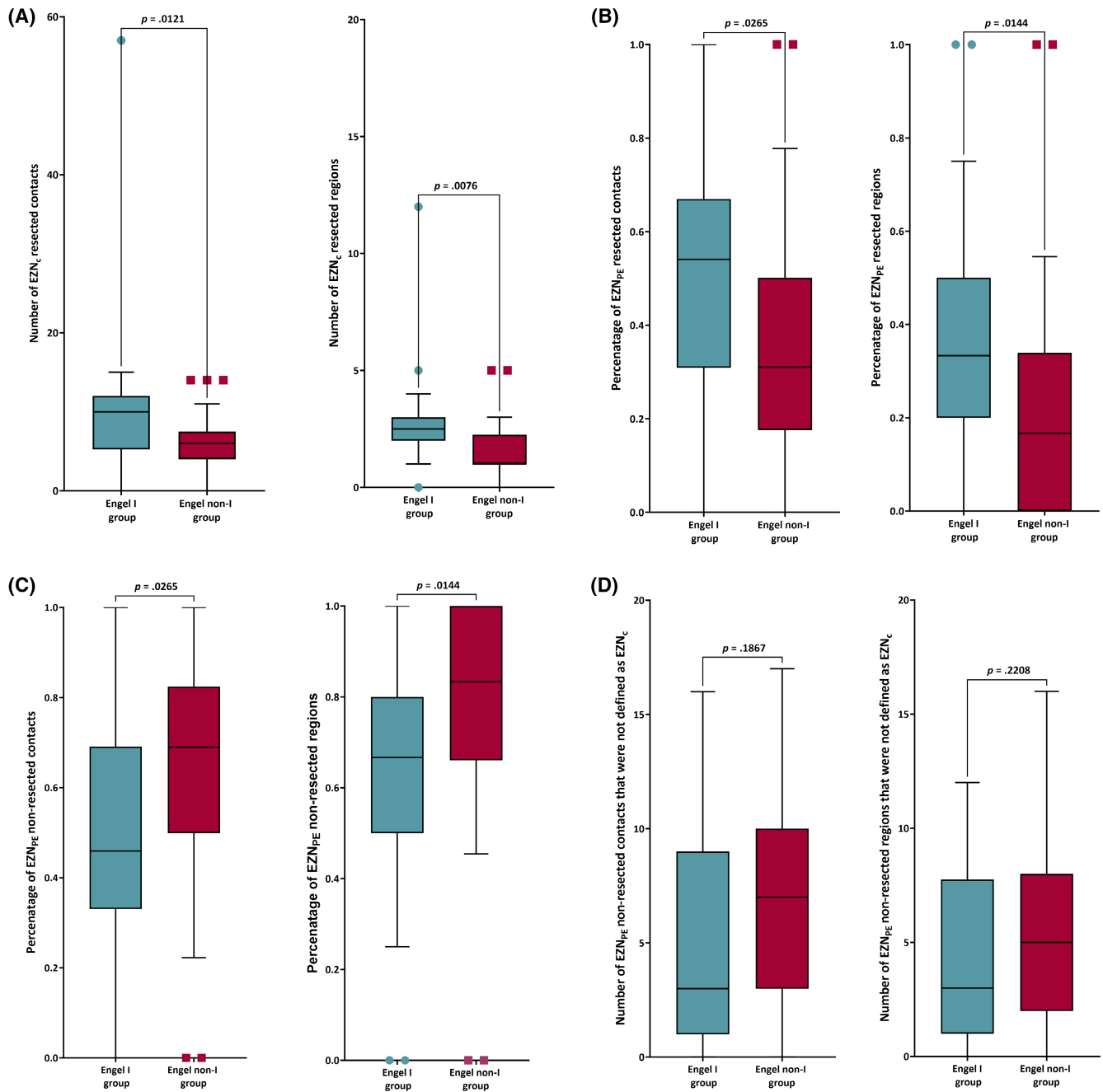


FIGURE 4 Permutation Entropy Index and the extent of the EZN resection according to surgical outcome. (A) The number of resected epileptogenic contacts and regions defined by clinical analysis incorporating the Epileptogenicity Index and the connectivity epileptogenicity index methods (EZN_c), was significantly higher in the Engel I group compared to the Engel non-I group. (B) The percentages of resected epileptogenic contacts and regions defined by the PEI (EZN_{PE}) were significantly higher in the Engel I group (PR-based threshold). (C) The percentage of non-resected EZN_{PE} contacts and regions was significantly higher in the Engel non-I group (PR-based threshold). (D) The number of non-resected epileptogenic contacts identified by the PEI, but not by clinicians (EZN_{PE} non-EZN_c) tended to be higher in the Engel non-I group compared to the Engel I group. EZN, Epileptogenic Zone Network; PEI, Permutation Entropy Index; PR, precision-recall.

in the EEG signal requires an equilibrium in entropy values to be informative.³⁰ Whatever the mechanism, the PEI combines these two characteristics of ictal/post-ictal dynamics.

To the best of our knowledge, only one study has used this type of approach to identify the epileptogenic

zone.⁴⁰ In this study, the authors used the low entropy properties of neuronal oscillations associated with spatially confined events in brain activity to estimate the location of the corresponding generators and to automatically predict the site of the “epileptic focus” based on the preictal-ictal period. The novelty of our study is

to integrate the postictal SEEG signal changes and to evaluate the performances of different PE-derived parameters in estimating the EZN. The EZN was defined by the clinical analysis incorporating two validated SEEG quantification methods (EI and cEI). The best performing PEDP was the normalized value of the ratio between the maximum postictal entropy and the minimum ictal entropy ($\frac{M}{m_{\max}}$), called here the “permutation entropy index.”

The PEI values showed a descending gradient from the EZN to the PZN and NIZ, demonstrating its ability to differentiate between these distinct regions. Because epilepsy surgery aims at removing or disconnecting the EZN, such discrimination is essential.

Concerning the seizure-onset patterns, PEI disclosed higher performance in identifying epileptogenic regions in patients experiencing seizures without low-voltage fast activity at seizure onset compared to those with fast SOP. This finding suggests that the PEI approach may complement more classical spectral approaches in this category of patients, which represented as much as 28% of cases in the present cohort.

Regarding the surgical prognosis, an important result of the present study is that the percentage of resected EZN contacts or regions defined by the PE correlated with surgical outcome and was significantly higher in seizure-free than in non-seizure-free patients. There was also a trend to a higher number of non-resected EZN contacts as defined by the PEI in non-seizure-free patients. A more detailed analysis of such cases is important to better understand the reasons for surgical failure in individual patients, since, despite the possibility of false-positive detections, some of these regions could be important hubs of the propagation network and thus potential targets for thermocoagulation or personalized neuromodulation approaches.

PE is easy to use computationally when applied in large data sets (203 seizures were analyzed, each trace having 82.5 ± 29.2 bipolar derivations). PE computation on a SEEG data set requires only a correct manual marking of the electrical seizure termination.

Among the limitations of our study are its retrospective design and the selection of patients undergoing curative surgery, whereas patients contraindicated for surgery were not included, with bias due to the sampling limited by the SEEG implantation, and VEP atlas parcellation subject to errors in cases where patient anatomy was severely distorted.

In conclusion, the PEI, evaluated with current clinical and quantification approaches, appears to be a promising tool for improving EZN delineation, which is a crucial goal for improving surgical strategies and outcomes after SEEG.

AUTHOR CONTRIBUTIONS

Ionut-Flavius Bratu: Conceptualization, Methodology, Data analysis, Validation, Visualization, Writing – Original Draft Preparation, Review & Editing. Julia Makhalova: Conceptualization, Methodology, Data analysis, Supervision, Validation, Writing – Original Draft Preparation, Review & Editing. Elodie Garnier: Data Curation and Analysis, Visualization. Samuel Medina: Data Curation, Software, Validation, Visualization. Aude Jegou: Data Curation, Software. Stanislas Lagarde: Acquisition of Data, Review & Editing. Francesca Pizzo: Acquisition of Data, Review & Editing. Agnes Trébuchon: Acquisition of Data, Review & Editing. Francesca Bonini: Acquisition of Data, Review & Editing. Didier Scavarda: Acquisition of Data, Review & Editing. Romain Carron: Acquisition of Data, Review & Editing. Christian Bénar: Conceptualization, Methodology, Supervision, Validation, Writing – Review & Editing. Fabrice Bartolomei: Conceptualization, Methodology, Supervision, Validation, Visualization, Writing – Original Draft Preparation, Review & Editing.

ACKNOWLEDGMENTS

We thank Maria Fratello, Christian Ferreyra, Nicolas Hemmer, and the entire DYNAMAP team for their help with the BIDS database; and Dr Sandrine Aubert, Dr Aileen McGonigal, Dr Lisa Vaugier, Dr Tanguy Madec, Dr Anne Lepine, and Dr Nathalie Villeneuve for the clinical management of some included patients.

FUNDING INFORMATION

This work was supported by the European Research Council: Galvani project, ERC-SyG 2019, grant agreement No 855109 and by the RHU EPINOV, A*MIDEX project (ANR-17-RHUS-0004) funded by the ‘Projet Investissements d’Avenir’ of the French Government.

CONFLICT OF INTEREST STATEMENT

None of the authors has any conflict of interest to disclose. We confirm that we have read the Journal’s position on issues involved in ethical publication and affirm that this report is consistent with those guidelines.

ORCID

Ionuț-Flavius Bratu  <https://orcid.org/0000-0002-8978-8927>

Julia Makhalova  <https://orcid.org/0000-0001-7962-2942>

Elodie Garnier  <https://orcid.org/0000-0003-2682-4369>

Stanislas Lagarde  <https://orcid.org/0000-0003-2916-1302>

Agnès Trébuchon  <https://orcid.org/0000-0002-8632-3454>

Didier Scavarda  <https://orcid.org/0000-0001-9344-8071>

Christian Bénar  <https://orcid.org/0000-0002-3339-1306>

Fabrice Bartolomei  <https://orcid.org/0000-0002-1678-0297>

REFERENCES

- Ryvlin P, Cross JH, Rheims S. Epilepsy surgery in children and adults. *Lancet Neurol.* 2014;13(11):1114–26.
- Cardinale F, Cossu M, Castana L, Casaceli G, Schiariti MP, Miserocchi A, et al. Stereoelectroencephalography: surgical methodology, safety, and stereotactic application accuracy in 500 procedures. *Neurosurgery.* 2013;72(3):353–66.
- Bancaud J, Angelergues R, Bernouilli C, Bonis A, Bordas-Ferrer M, Bresson M, et al. Functional stereotaxic exploration (stereoelectroencephalography) in epilepsies. *Rev Neurol (Paris).* 1969;120(6):448.
- Stefan H, Lopes da Silva FH. Epileptic neuronal networks: methods of identification and clinical relevance. *Front Neurol.* 2013;4:8.
- Bartolomei F, Lagarde S, Wendling F, McGonigal A, Jirsa V, Guye M, et al. Defining epileptogenic networks: contribution of SEEG and signal analysis. *Epilepsia.* 2017;58:1131–47.
- Bartolomei F, Nica A, Valenti-Hirsch MP, Adam C, Denuelle M. Interpretation of SEEG recordings. *Neurophysiol Clin.* 2018;48(1):53–7.
- Bartolomei F, Chauvel P, Wendling F. Epileptogenicity of brain structures in human temporal lobe epilepsy: a quantified study from intracerebral EEG. *Brain.* 2008;131(7):1818–30.
- Balatskaya A, Roehri N, Lagarde S, Pizzo F, Medina S, Wendling F, et al. The “Connectivity Epileptogenicity Index” (cEI), a method for mapping the different seizure onset patterns in StereoElectroEncephalography recorded seizures. *Clin Neurophysiol.* 2020;131(8):1947–55.
- David O, Blauwblomme T, Job A-S, Chabardès S, Hoffmann D, Minotti L, et al. Imaging the seizure onset zone with stereoelectroencephalography. *Brain.* 2011;134(10):2898–911.
- Gnatkovsky V, de Curtis M, Pastori C, Cardinale F, Lo Russo G, Mai R, et al. Biomarkers of epileptogenic zone defined by quantified stereo-EEG analysis. *Epilepsia.* 2014;55(2):296–305.
- Grinenko O, Li J, Mosher JC, Wang IZ, Bulacio JC, Gonzalez-Martinez J, et al. A fingerprint of the epileptogenic zone in human epilepsies. *Brain.* 2018;141(1):117–31.
- Lagarde S, Buzori S, Trebuchon A, Carron R, Scavarda D, Milh M, et al. The repertoire of seizure onset patterns in human focal epilepsies: determinants and prognostic values. *Epilepsia.* 2019;60(1):85–95.
- Perucca P, Dubeau F, Gotman J. Intracranial electroencephalographic seizure-onset patterns: effect of underlying pathology. *Brain.* 2014;137(Pt 1):183–96.
- Cardinale F, Rizzi M, Vignati E, Cossu M, Castana L, d’Orio P, et al. Stereoelectroencephalography: retrospective analysis of 742 procedures in a single Centre. *Brain.* 2019;142(9):2688–704.
- Jehi L, Morita-Sherman M, Love TE, Bartolomei F, Bingham W, Braun K, et al. Comparative effectiveness of stereotactic electroencephalography versus subdural grids in epilepsy surgery. *Ann Neurol.* 2021;90(6):927–39.
- Courtens S, Colombet B, Trébouchon A, Brovelli A, Bartolomei F, Bénar CG. Graph measures of node strength for characterizing preictal synchrony in partial epilepsy. *Brain Connect.* 2016;6(7):530–9.
- Kahane P, Landré E, Minotti L, Francione S, Ryvlin P. The Bancaud and Talairach view on the epileptogenic zone: a working hypothesis. *Epileptic Disord.* 2006;8 Suppl 2:S16–26.
- Buccellato A, Çatal Y, Bisiacchi P, Zang D, Del FA, Mao Y, et al. Probing intrinsic neural timescales in EEG with an information-theory inspired approach: permutation entropy time delay estimation (PE-TD). *Entropy.* 2023;10(25):1086.
- Iasemidis LD, Chris Sackellares J, Zaveri HP, Williams WJ. Phase space topography and the Lyapunov exponent of electrocorticograms in partial seizures. *Brain Topogr.* 1990;2(3):187–201.
- Isnard J, Taussig D, Bartolomei F, Bourdillon P, Catenox H, Chassoux F, et al. French guidelines on stereoelectroencephalography (SEEG). *Neurophysiol Clin.* 2018;48:5–13.
- Makhalova J, Medina Villalon S, Wang H, Giusiano B, Woodman M, Bénar C, et al. Virtual epileptic patient brain modeling: relationships with seizure onset and surgical outcome. *Epilepsia.* 2022;63(8):1942–55.
- Scavarda D, Cavalcante T, Trébouchon A, Lépine A, Villeneuve N, Girard N, et al. Tailored supratentorial partial hemispherotomy: a new functional disconnection technique for stroke-induced refractory epilepsy. *J Neurosurg Pediatr.* 2018;22(6):601–9.
- Colombet B, Woodman M, Badier JM, Bénar CG. AnyWave: a cross-platform and modular software for visualizing and processing electrophysiological signals. *J Neurosci Methods.* 2015;242:118–26.
- Medina Villalon S, Paz R, Roehri N, Lagarde S, Pizzo F, Colombet B, et al. EpiTools, a software suite for presurgical brain mapping in epilepsy: intracerebral EEG. *J Neurosci Methods.* 2018;303:7–15.
- Wang HE, Scholly J, Triebkorn P, Sip V, Medina Villalon S, Woodman MM, et al. VEP atlas: an anatomic and functional human brain atlas dedicated to epilepsy patients. *J Neurosci Methods.* 2021;348:108983.
- Yang Y, Zhou M, Niu Y, Li C, Cao R, Wang B, et al. Epileptic seizure prediction based on permutation entropy. *Front Comput Neurosci.* 2018;19:12.
- El Youssef N, Jegou A, Makhalova J, Naccache L, Bénar C, Bartolomei F. Consciousness alteration in focal epilepsy is related to loss of signal complexity and information processing. *Sci Rep.* 2022;12(1):22276.
- Chatzikonstantinou S, Jegou A, Brohée S, Singh R, Bénar C, Lagarde S, et al. How may a brief seizure lead to prolonged epileptic amnesia? *Brain Topogr.* 2023;36(2):129–34.
- Shannon CE. A mathematical theory of communication. *Bell Syst Tech J.* 1948;27(3):379–423.
- Bandt C, Pompe B. Permutation entropy: a natural complexity measure for time series. *Phys Rev Lett.* 2002;88(17):174102.
- Henry M, Judge G. Permutation entropy and information recovery in nonlinear dynamic economic time series. *Econometrics.* 2019;7(1):10.
- Unakafova V, Keller K. Efficiently measuring complexity on the basis of real-world data. *Entropy.* 2013;15(12):4392–415.
- Makhalova J, Madec T, Medina Villalon S, Jegou A, Lagarde S, Carron R, et al. The role of quantitative markers in surgical prognostication after stereoelectroencephalography. *Ann Clin Transl Neurol.* 2023;10:2114–26.

34. R Core Team. A language and environment for statistical computing. Vienna, Austria: R Foundation for Statistical Computing; 2022. <https://www.r-project.org/>
35. Iasemidis LD, Shiau D-S, Sackellares JC, Pardalos PM, Prasad A. Dynamical resetting of the human brain at epileptic seizures: application of nonlinear dynamics and global optimization techniques. *IEEE Trans Biomed Eng.* 2004;51(3):493–506.
36. Bruzzo AA, Gesierich B, Santi M, Tassinari CA, Birbaumer N, Rubboli G. Permutation entropy to detect vigilance changes and preictal states from scalp EEG in epileptic patients. A preliminary study. *Neurol Sci.* 2008;29(1):3–9.
37. Ferlazzo E, Mammone N, Cianci V, Gasparini S, Gambardella A, Labate A, et al. Permutation entropy of scalp EEG: a tool to investigate epilepsies. *Clin Neurophysiol.* 2014;125(1):13–20.
38. Lehnertz K, Elger CE. Spatio-temporal dynamics of the primary epileptogenic area in temporal lobe epilepsy characterized by neuronal complexity loss. *Electroencephalogr Clin Neurophysiol.* 1995;95(2):108–17.
39. Pijn JP, Van Neerven J, Noest A, Lopes da Silva FH. Chaos or noise in EEG signals; dependence on state and brain site. *Electroencephalogr Clin Neurophysiol.* 1991;79(5):371–81.
40. Vila-Vidal M, Pérez Enríquez C, Principe A, Rocamora R, Deco G, Tauste Campo A. Low entropy map of brain oscillatory activity identifies spatially localized events: a new method for automated epilepsy focus prediction. *Neuroimage.* 2020;208:116410.

SUPPORTING INFORMATION

Additional supporting information can be found online in the Supporting Information section at the end of this article.

How to cite this article: Bratu I-F, Makhalova J, Garnier E, Villalon SM, Jegou A, Bonini F, et al. Permutation entropy-derived parameters to estimate the epileptogenic zone network. *Epilepsia.* 2024;65:389–401. <https://doi.org/10.1111/epi.17849>